Dalton Transactions

ROYAL SOCIETY OF CHEMISTRY

PAPER

View Article Online
View Journal | View Issue

Check for updates

Cite this: *Dalton Trans.*, 2024, **53**, 10901

Hydroxopalladium(IV) complexes prepared using oxygen or hydrogen peroxide as oxidants†

Ava Behnia, Mahmood A. Fard, Johanna M. Blacquiere * and Richard J. Puddephatt *

Received 23rd April 2024,
Accepted 12th June 2024

DOI: 10.1039/d4dt01202j

rsc.li/dalton

Published on 13 Haziran 2024. Downloaded on 8.08.2024 12:38:59.

The cycloneophylpalladium(II) complexes [Pd($CH_2CMe_2C_6H_4$)(κ^2-*N*,*N*′-**L**)], **1** or **2**, with **L** = RO$(CH_2)_3$N$(CH_2$-2-$C_5H_4N)_2$, with R = H or Me, respectively, react with either dioxygen or hydrogen peroxide in the presence of $NH_4[PF_6]$ to give rare examples of the corresponding hydroxopalladium(IV) complexes [Pd(OH)($CH_2CMe_2C_6H_4$)(κ^3-*N*,*N*′,*N*″-**L**)][PF_6], **3** or **4**. The complexes **3** and **4** are stable at room temperature and have been structurally characterized. On heating a solution of **3** or **4** in moist dimethylsulphoxide, selective reductive elimination with C(sp^2)–O bond formation is observed, followed by hydrolysis, to give the corresponding pincer complex [Pd(OH)(κ^3-*N*,*N*′,*N*″-**L**)][PF_6] and 2-*t*-butylphenol as major products. A more complex reaction occurs in chloroform solution. The mechanisms of reaction are discussed, supported by DFT calculations.

1. Introduction

There is much current interest in the palladium catalyzed oxidative functionalization of alkanes and arenes as a versatile tool in organic synthesis.[1–6] To introduce oxygen-containing functional groups, the use of the inexpensive, environmentally friendly oxidants dioxygen or hydrogen peroxide is ideal, but remains challenging for many applications.[1–9] Palladium(IV) complexes have been proposed as intermediates in some catalytic C–H bond functionalization reactions using O_2 or H_2O_2 as an oxidant.[10–13] Some examples are illustrated in Scheme 1(a),[10] 1(b),[11] and 1(c).[12]

A useful approach in developing this important field of research is to study the stoichiometric reactions of oxygen or hydrogen peroxide with organopalladium compounds to test what is possible in the potential steps of a catalytic cycle.[14–19] For example, oxo or hydroxo complexes of palladium(IV) have been proposed as short-lived intermediates in oxygen atom insertion reactions using peroxide reagents (Scheme 2). Thus, complex ***A*** reacted with *t*-BuOOH to give ***C***, perhaps *via* the oxopalladium(IV) complex ***B***,[15] while ***D*** reacted with hydrogen peroxide to give ***F***, perhaps *via* the hydroxopalladium(IV) complex ***E***.[16] The precedents have all been shown to involve 2-electron mechanisms involving Pd(II)–Pd(IV) complexes,[14–19] rather than the 1-electron mechanisms often found in related bioinorganic systems.[20–23]

Most hydroxopalladium(IV) complexes have been proposed as reaction intermediates, but a few have been isolated, all of which contain *fac*-tridentate ligands.[22–27] The first example was a triazolylborate complex ***H***, formed by oxidation of the palladium(II) precursor ***G*** (Scheme 3a).[22] Similarly, oxidation of palladium(II) precursor ***I*** gave the palladium(IV) derivative ***J***, which underwent selective reductive elimination with C(sp^2)–O bond formation on heating to give 2-*t*-butylphenol

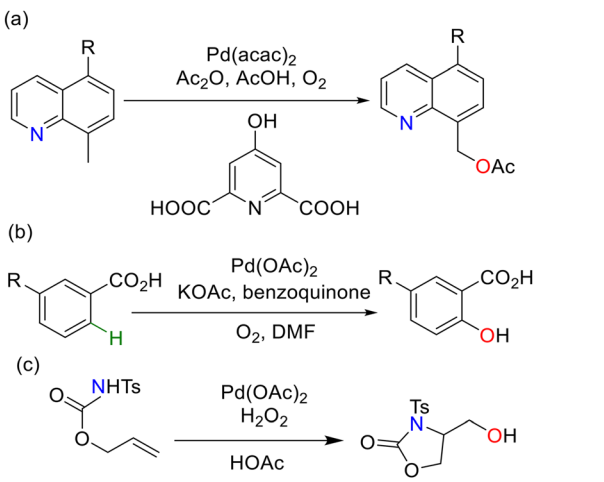

Scheme 1 Pd-catalyzed C–H functionalization reactions with O_2 or H_2O_2 as oxidants.

Department of Chemistry, University of Western Ontario, London, Canada N6A 5B7. E-mail: johanna.blacquiere@uwo.ca, pudd@uwo.ca

†Electronic supplementary information (ESI) available: Figures S1–S14 (NMR spectra), Fig. S15–S17 (X-ray structures), Table S1 (X-ray data), Fig. S18–S20 (DFT calculated structures and ground state energies). CCDC 2091353, 2091354 and 2334979. For ESI and crystallographic data in CIF or other electronic format see DOI: https://doi.org/10.1039/d4dt01202j

Published on 13 Haziran 2024. Downloaded on 8.08.2024 12:38:59.

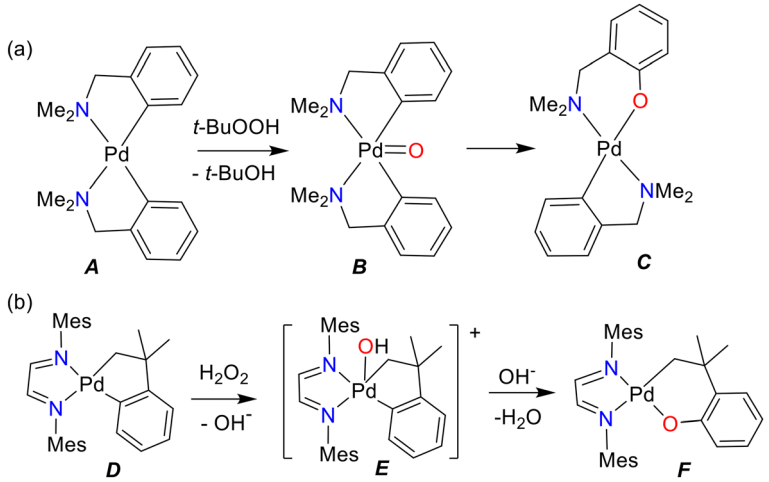

Scheme 2 Oxygen-atom insertion into the Pd–C bond, with proposed Pd(IV) oxo/hydroxo intermediates, ***B*** and ***E***.

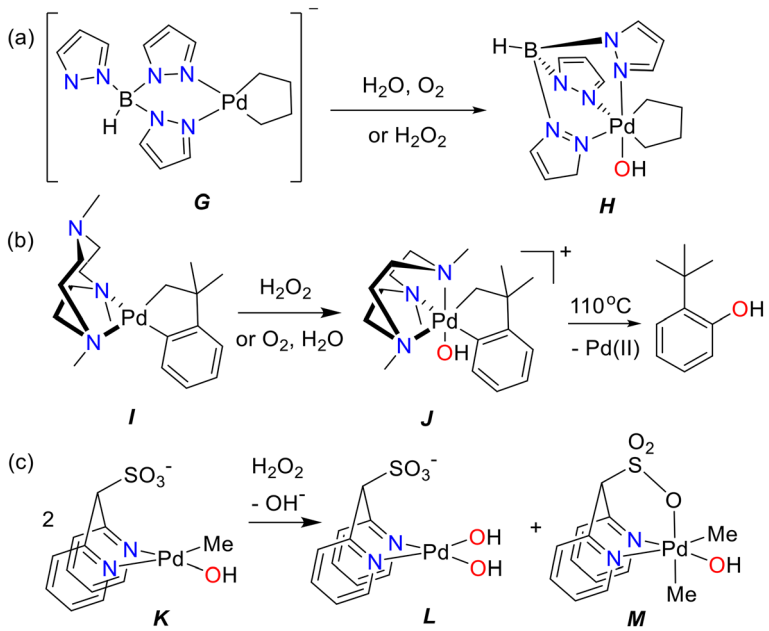

Scheme 3 Some known hydroxopalladium(IV) complexes.

(Scheme 3b).[23] Even a monoalkyl palladium(II) complex could be oxidized, with subsequent methyl group exchange, by using a ligand with a pendent sulfonate group (Scheme 3c).[24] Most known hydroxo complexes of palladium are in oxidation state Pd(II) and these complexes have been studied in depth.[26–29]

The ligands in complexes ***G–M*** (Scheme 3) showcase that hemilabile ligands, that toggle between bidentate and tridentate coordination modes, can stabilize both Pd(II) and Pd(IV) complexes. The hemilabile ligands $RO(CH_2)_3N(CH_2\text{-}2\text{-}C_5H_4N)_2$, **L1**, R = H, or **L2**, R = Me,[30,31] and their cycloneophylpalladium (II) complexes **1** and **2** (Scheme 4) have been reported previously.[32–36] The preferred isomers exhibit bidentate ligand coordination with a 5-membered chelate.[34–36] The major isomers, **1a** or **2a**, have the aryl group *trans* to the pyridyl donor, structures which are slightly lower in energy than **1b** or **2b** with the aryl group *trans* to the tertiary amine donor. The complexes exhibit fluxionality in solution at room temperature and all three of the square planar isomers (Scheme 3) are thermally accessible.[34–36] By analogy with the reactions of Scheme 3, the complexes **1** and **2** were expected to react with H_2O_2 or with O_2/H_2O to give relatively stable palladium(IV) complexes in which **L1** or **L2** acts as a tridentate ligand. In addition, the alcohol group in complex **1** might provide extra reactivity by hydrogen bonding to the incoming reagent (**L1** may act as a push–pull ligand).[37,38] This assistance through the second coordination sphere would be viable only *via* reac-

 This journal is © The Royal Society of Chemistry 2024

Published on 13 Haziran 2024. Downloaded on 8.08.2024 12:38:59.

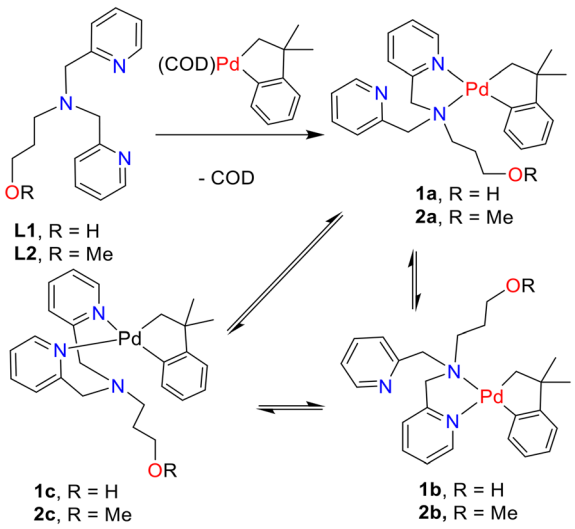

Scheme 4 The synthesis of cycloneophylpalladium(II) complexes **1** and **2** (COD = 1,5-cyclooctadiene).

tion of isomers **1a** or **1b**, within which the pendent alcohol substituent is positioned *cis* to one of the open sites on palladium.

This article reports new examples of the oxidation using the green oxidants O_2 or H_2O_2, of cycloneophylpalladium(II) complexes **1** and **2**, which are supported by the easily synthesized tridentate N-donor ligands **L1** and **L2**. Then the reductive elimination reactions of the hydroxopalladium(IV) complexes are reported.

2. Results and discussion

2.1. Synthesis and structure of hydroxopalladium(IV) complexes

A solution of [Pd($CH_2CMe_2C_6H_4$)(κ^2-*N*,*N*′-**L1**)], **1**, in methanol is orange in color, and it fades with concomitant formation of a yellow precipitate when exposed to O_2 in the presence of $NH_4[PF_6]$ (Scheme 5). The precipitated product is [Pd(OH)($CH_2CMe_2C_6H_4$)(κ^3-*N*,*N*′,*N*″-**L1**)][PF_6], **3**, which is also formed in wet chloroform solution, or by reaction of **1** with aqueous hydrogen peroxide. As a control experiment to test if the alcohol functionality in complex **1** played a significant role in these transformations, analogous reactions with [Pd($CH_2CMe_2C_6H_4$)(κ^2-*N*,*N*′-**L2**)], **2**, were carried out. Very similar reactivity was observed, and the complex [Pd(OH)($CH_2CMe_2C_6H_4$)(κ^3-*N*,*N*′,*N*″-**L2**)][PF_6], **4**, was formed on reaction of **2** with either O_2 or H_2O_2 in methanol solution in the presence of $NH_4[PF_6]$ (Scheme 5). The new hydroxopalladium (IV) complexes **3** and **4** were isolated in yields of 71% and 62% respectively from the reactions with dioxygen and they could be stored at −5 °C as solid samples for over a month, and were stable in solution in dmso-d_6 for several days at room temperature. Complexes **3** and **4** are rare examples of hydroxopalladium(IV) complexes, especially those formed by oxidative addition using hydrogen peroxide or oxygen as oxidants.[22–27,39]

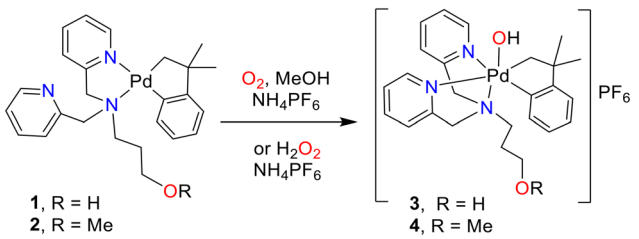

Scheme 5 The synthesis of complexes **3** and **4**, using dioxygen or hydrogen peroxide as oxidant.

The complexes **3** and **4** were fully characterized by structure determinations and by ^1H and ^{13}C NMR spectroscopy, including correlated ^1H–^1H COSY, and ^1H–^{13}C HSQC and HMBC NMR spectroscopy. The ^1H NMR spectrum of complex **3** in dmso-d_6 showed 12 distinct aromatic signals in the range δ 6.61–8.71, and four different doublet resonances at δ 4.92, 4.62, 4.58 and 4.52 for methylene protons of the pyCH_2N groups. For the cycloneophyl group, the CMe_2 and CH_2 groups each gave two distinct resonances. These NMR spectroscopy data, and the similar data for complex **4**, indicate the presence of a single isomer with no symmetry in each case, but the stereochemistry is not defined.

The solid-state structures of complexes **3** and **4** were determined and are shown in Fig. 1–3. Complex **3** crystallized in the monoclinic space group $P2_1/n$ and so the lattice contains both enantiomers of the asymmetric octahedral complex (Fig. 1). In contrast, complex **4** crystallized in the chiral space group

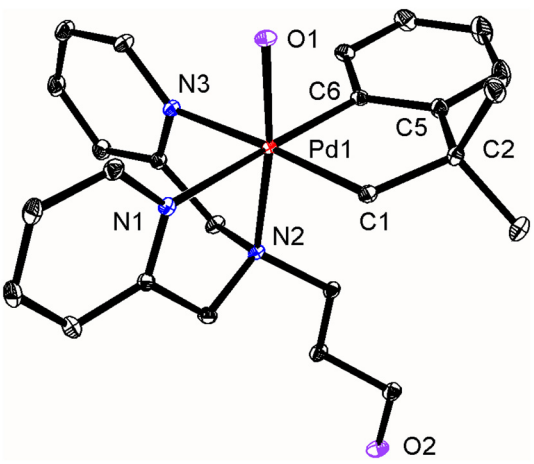

Fig. 1 The structure of complex **3**, showing 30% ellipsoids for the clockwise enantiomer **3C**. Hydrogen atoms and the PF_6^- counterion were removed for clarity. Selected bond parameters: Pd(1)C(1) 2.0539 (13), Pd(1)C(6) 1.9915(12), Pd(1)O(1) 1.9963(12), Pd(1)N(1) 2.1356(12), Pd(1)N(2) 2.1393(12), Pd(1)N(3) 2.1908(12) Å; C(6)Pd(1)C(1) 83.33(5), O(1)Pd(1)N(2) 172.59(3), N(1)Pd(1)N(2) 82.14(4), N(1)Pd(1)N(3) 83.17(5), N(2)Pd(1)N(3) 80.53(4)°.

Published on 13 Haziran 2024. Downloaded on 8.08.2024 12:38:59.

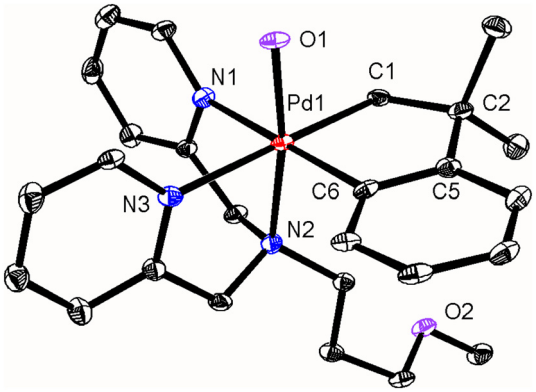

Fig. 2 Structure of the anticlockwise enantiomer of complex **4A**, showing 30% probability ellipsoids. Hydrogen atoms and the PF_6^- counterion were removed for clarity. Selected bond parameters: Pd(1)C(1) 2.040(8), Pd(1)C(6) 1.979(8), Pd(1)O(1) 1.990(6), Pd(1)N(1) 2.136(8), Pd(1)N(2) 2.151(8), Pd(1)N(3) 2.185(8) Å; C(6)Pd(1)C(1) 83.4(4), O(1)Pd(1)N(2) 171.4(3), N(1)Pd(1)N(2) 81.9(3), N(1)Pd(1)N(3) 83.4(3), N(2)Pd(1)N(3) 80.5(3)°.

$P2_12_12_1$ and the lattice contains a single enantiomer (Fig. 2). In each case, the palladium(IV) center has octahedral stereochemistry with the two pyridyl groups *trans* to carbon donors and the amine group *trans* to the hydroxo ligand. This stereochemistry is expected if the oxidative addition occurs from the *least* stable isomer of complex **1** or **2**, namely **1c** or **2c** (Scheme 4). Thus, if the reagent approaches on one side of the square plane of palladium(II) and the free nitrogen donor coordinates on the opposite side, only isomer **1c** or **2c** would give **3** or **4**, respectively. The bond distances and angles in **3** and **4** are unexceptional (Fig. 1 and 2).[22,23]

In the solid-state, the PdOH group in complex **4** does not take part in hydrogen bonding. However, there is significant intermolecular hydrogen bonding in complex **3** leading to formation of supramolecular polymeric chains (Fig. 3). The distance of O(1)–O(2A) = 2.78(1) Å corresponds to a moderate strength hydrogen bond.[40] Individual polymer chains are formed through self-recognition and contain molecules of the same chirality (isotactic), and there are equal numbers of polymer chains containing complex **3** with the C (clockwise) or A (anticlockwise) chirality.

2.2. Reductive elimination reactions of hydroxopalladium(IV) complexes

Initial studies of reductive elimination indicated similar reactivity of complexes **3** and **4**, thus there was no evidence to suggest the pendant OH group alters the reactivity as has been observed by others.[37,38] Since the polymeric complex **3** had very limited solubility it was difficult to study, so the more detailed experiments were carried out using **4**. Reactions were studied in chloroform and in dmso-d_6 solution. At the temperatures needed to induce reductive elimination, no organopalladium intermediates were observed, but only palladium(II) complexes and organic products were identified.

The decomposition reaction of complex **4** in dmso-d_6, as monitored by ^{1}H NMR spectroscopy, was relatively simple, giving the palladium(II) complex [Pd(OH)(**L2**)][PF_6], **5**, and 2-*t*-butylphenol (**BP**) as the major organic product, along with some of the benzocyclobutane derivative **BCB**, according to Scheme 6(i). These products are analogous to those formed from the hydroxopalladium(IV) complex ***J***, which is supported by a tridentate NNN donor ligand without a pendent OH/OR group (Scheme 3).[23] The similar stability of Pd–OH complexes **3**, **4** and ***J***, and the selectivity for the same neophyl oxidation product, suggests that the pendent OH/OMe groups in complexes **3** and **4** play a negligible role in the oxidation chemistry. The formation of 2-*t*-butylphenol (**BP**) involves hydrolysis of an initially formed palladium(II) product by adventitious water present in the solvent. The formation of **BP** from **4** likely follows the same pathway, and this was confirmed through calculations (*vide infra*).

The decomposition of complex **4** in chloroform was more complex, with additional observed organic products and generation of the known palladium(II) product [PdCl(**L2**)][PF_6], **6**,[34] which implicates reaction with the solvent (Scheme 6(ii)). Complex **4** was not sufficiently soluble in $CDCl_3$ to allow monitoring of organic and inorganic products by ^{1}H NMR spectroscopy. Instead, the organic products were analyzed by GC-MS following reductive elimination of **4** in $CHCl_3$ at 55 °C, removal of aliquots during reaction, and separation of palladium complexes by filtration through a silica plug. For each aliquot, the residual solvent was removed under vacuum to give the palladium(II) product **6**, in which the chloride ligand must be installed by reaction with the solvent chloroform. The

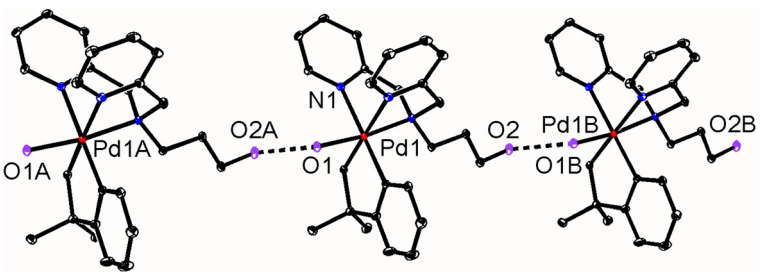

Fig. 3 The supramolecular polymeric structure of complex **3C**. Equivalent atoms: *x*, *y*, *z*; *x*, *y* + 1, *z*; *x*, *y* − 1, *z*. H-bond distance: O(1)···(O(2A) = O(2)···O(1B) = 2.78(1) Å.

This journal is © The Royal Society of Chemistry 2024

Published on 13 Haziran 2024. Downloaded on 8.08.2024 12:38:59.

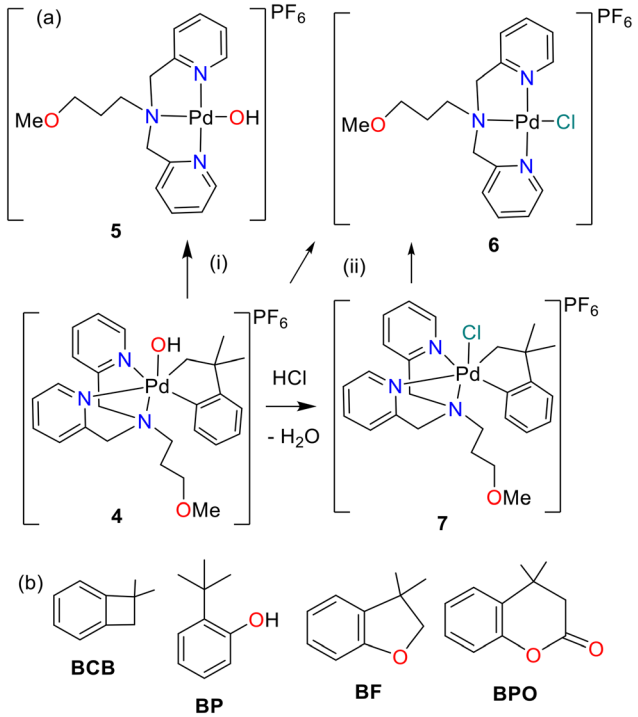

Scheme 6 Reductive elimination from complex **4**; (a) palladium complexes; (b) organic products; (i) reaction in dmso-d_6 at 105 °C for 1 h., – **BP** (90%), – **BCB** (4%); (ii) reaction in $CDCl_3$ at 55 °C for 8 h., – **BF** (1%), – **BP** (23%), – **BCB** (23%), – **BPO** (53%).

composition of the organic products varied with time, with the major product being **BP** in the early stages and **BPO** and **BCB** in the later stages. Scheme 6 gives the final composition. The formation of **BP** likely occurs directly from **4** following the same mechanism as occurs in dmso-d_6. While the mechanistic details are not known, the formation of **BPO** would require a carbonyl insertion step. Chloroform is well known to act as a source of CO and HCl by hydrolysis.[41] Thus, we propose HCl converts Pd–OH in **4** to a Pd–Cl moiety, and this intermediate could account for both **BPO** and **BCB**. We previously demonstrated that an analogous Pd(IV) bromide complex undergoes reductive elimination to form **BCB**.[36] We found that attempted recrystallization of complex **4** from $CHCl_3$/ether occurred with reaction to give the chloropalladium(IV) complex [PdCl($CH_2CMe_2C_6H_4$)(κ^3-*N*,*N*′,*N*″-**L2**)][PF_6], **7** (Fig. 4).

2.3. Insights from DFT calculations

To gain insight into the above reactions, some DFT calculations were carried out (see Experimental section for details). Initial calculations were carried out on products from complex **1**, containing ligand **L1**. Ground state structures were readily optimized (Fig. S18–S20†), but transition states were not, evidently because of the presence of the flexible $(CH_2)_3OH$ substituents. Since the complexes with $(CH_2)_3OH$ and $(CH_2)_3OMe$ substituents gave similar reactivity, the more detailed transition state calculations were carried out using the model *N*-methyl ligand $MeN(CH_2\text{-}2\text{-}C_5H_4N)_2$, **L**′. The ground state

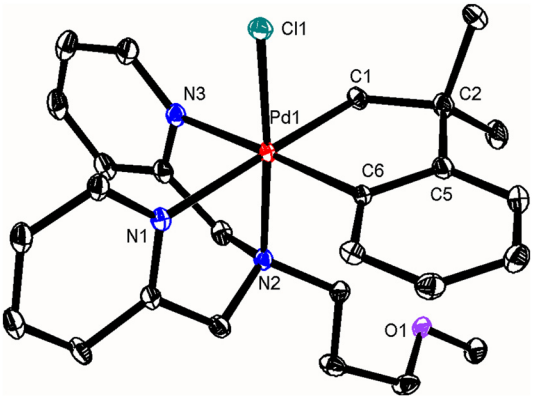

Fig. 4 The structure of the clockwise enantiomer of complex **7C**, showing 30% probability ellipsoids. Selected bond parameters: Pd(1)C(1) 2.059(4), Pd(1)C(6) 1.998(4), Pd(1)Cl(1) 2.2916(12), Pd(1)N(1) 2.199(3), Pd(1)N(2) 2.140(3), Pd(1)N(3) 2.158(3) Å; C(6)Pd(1)C(1) 83.27(15), Cl(1)Pd(1)N(2) 174.83(9), N(1)Pd(1)N(2) 81.05(11), N(1)Pd(1)N(3) 82.33(12), N(2)Pd(1)N(3) 82.19(12)°.

structure of **1**′ (a model for either **1** or **2**) is calculated to be **1a**′, with the amine donor *trans* to CH_2, but the isomers **1b**′ and **1c**′ are easily accessible by reversible pyridyl for amine exchange by way of 5-coordinate transition states (Fig. 5). The direct pyridyl for pyridyl exchange is calculated to have a much higher barrier. The fluxionality of complexes **1** and **2** is readily understood by this model. These results are consistent with our previous calculations of only two isomers of **1**, which showed the structure analogous to **1a**′ is more stable than that of **1b**′ by *ca.* 7 kJ mol^{-1}.[34] It proved possible to calculate the activation energy for the isomerization of isomers **1a**′ and **1c**′ with ligands $RN(CH_2\text{-}2\text{-}C_5H_4N)_2$, with R = Me, Et, Pr, Bu and $(CH_2)_3OH$, and these were respectively 27, 20, 20, 23 and 22 kJ mol^{-1}. The similarity of these values validates the use of the *N*-methyl ligand **L**′ as a model for **L1** and **L2** in subsequent calculations. It is well known that the tertiary amines are poorer ligands than secondary or primary amines, since the increased steric effects associated with addition of the third alkyl group outweigh the advantage of the donor ability of the alkyl group.[42–44]

As in related reactions,[23,30,31] the oxidative addition of hydrogen peroxide is predicted to occur by nucleophilic attack by the Pd(II) centre at the σ*(OO) orbital of H_2O_2 and is illustrated in Fig. 6. The easiest reaction is with the least stable isomer **1c**′, and is aided by anchimeric assistance for the S_N2 reaction by the amine donor group. Once the rearrangement of **1a**′ to **1c**′ has occurred and hydrogen peroxide approaches the palladium(II) center, the reaction occurs very easily. Without solvent involvement, the leaving hydroxide group remains strongly hydrogen bonded to the PdOH group in both the first formed intermediate ***N*** and in the product **3**′ (Fig. 6). There is predicted to be a small barrier to rearrangement of ***N*** to **3**′ (Fig. 6). In the real solution, hydrogen bonding to water molecules in the aqueous H_2O_2 reagent is likely to occur at each stage but, in either case, the reaction is predicted to occur rapidly, in agreement with experiment.

Published on 13 Haziran 2024. Downloaded on 8.08.2024 12:38:59.

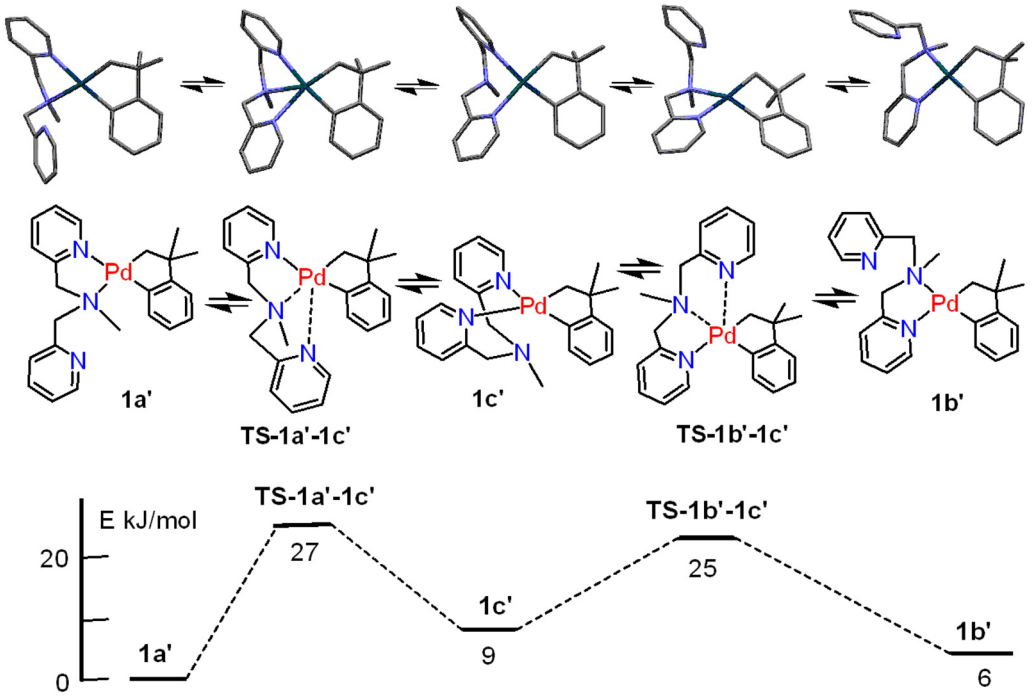

Fig. 5 The calculated mechanism and energetics of interconversion of isomers of complex **1'**.

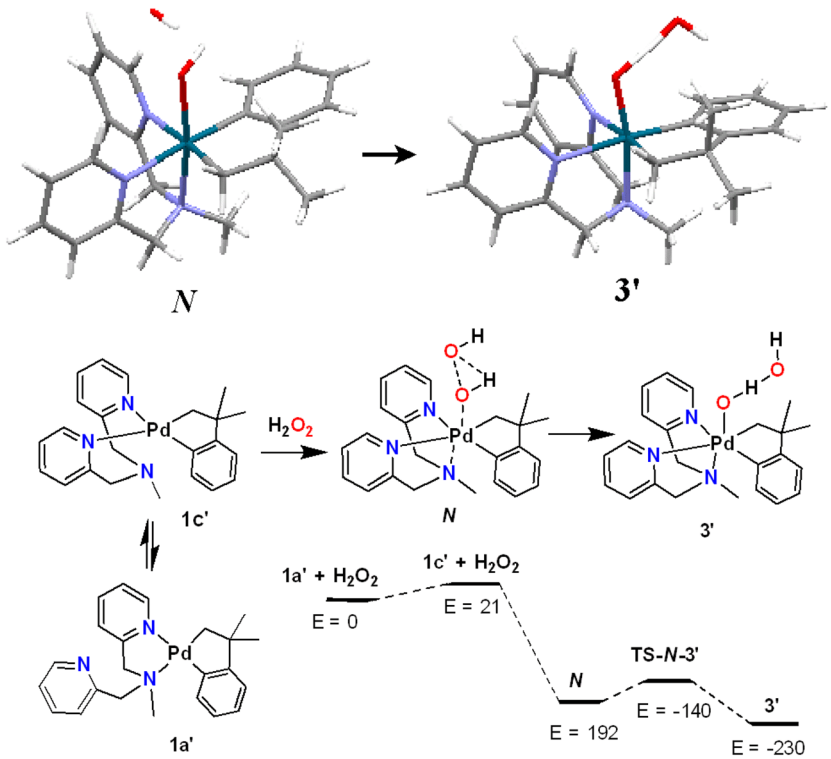

Fig. 6 The calculated structures and relative energies (E, kJ mol^{-1}) for reactions of complex **1'** with hydrogen peroxide. Calculated distances in ***N***, Pd–O 2.09, O–O 2.40, Pd–N(amine) 2.41 Å; TS-***N*-3'**, Pd–O 2.10, O–O 2.57, Pd–N(amine) 2.35 Å; **3'**, Pd–O 2.01, Pd–N(amine) 2.25 Å.

The reaction with dioxygen is expected to occur in two steps, first to give a hydroperoxide complex of palladium(IV) and then, by a further rapid reaction with Pd(II), to give two equivalents of the hydroxopalladium(IV) product.[45–49] This second step is expected to occur by the mechanism analogous to that with hydrogen peroxide (Scheme 6),[48,49] so only the

 This journal is © The Royal Society of Chemistry 2024

Published on 13 Haziran 2024. Downloaded on 8.08.2024 12:38:59.

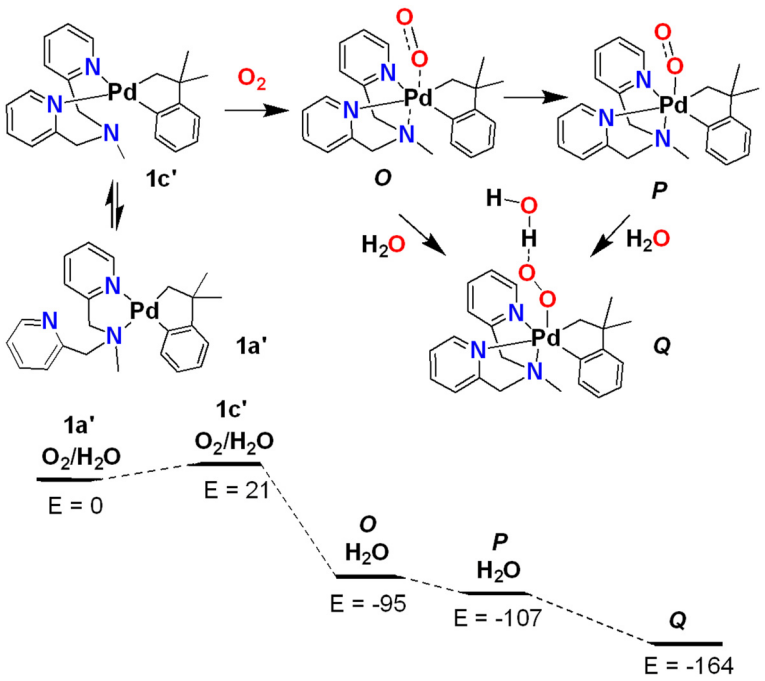

Fig. 7 The calculated structures and relative energies (*E*, kJ mol^{-1}) for reactions of complex **1′** with dioxygen. Calculated distances in ***O*-*t***, Pd–O 2.32, O–O 1.43, Pd–N(amine) 2.46 Å; ***O*-*s***, Pd–O 2.36, O–O 1.49, Pd–N(amine) 2.45 Å; ***P***, Pd–O 2.09, O–O 1.50, Pd–N(amine) 2.33 Å; ***Q***, Pd–O 2.09, O–O 1.51, Pd–N(amine) 2.24 Å.

first reaction with dioxygen is discussed here. The initial reaction of complex **1′** with dioxygen is shown in Fig. 7. As with the reaction with hydrogen peroxide (Fig. 6) an initial rearrangement of isomer **1a′** to **1c′** is followed by facile reaction with O_2. At longer Pd···O distances, the triplet state is more stable and the crossover to the singlet state occurs when Pd···O is about 2.35 Å at ***O*** in Fig. 7, before giving the singlet η^1-dioxygen complex ***P***. This reaction profile is similar to that calculated for the reaction of complexes $L_2Pd(0)$ with dioxygen although, in that case, a further rearrangement to the stable η^2-peroxide complex $[L_2Pd(O_2)]$ is observed.[50–52] In the presence of water, as a model for the hydroxylic solvent, a further stabilization of the more polar singlet state is predicted to give the incipient hydroperoxide complex ***Q*** (Fig. 7), and then further facile reaction with **1c′** can give **3′** in a similar way as in the reaction of **1c′** with hydrogen peroxide (Fig. 6).

A possible mechanism for the reductive elimination from the model hydroxopalladium(IV) complex **3′** is shown in Fig. 8. Initially, several mechanisms were studied, involving direct reductive elimination from **3′** or its isomers or involving reductive elimination from a 5-coordinate intermediate formed by dissociation of one of the nitrogen donor ligands from **3′**, as found in other concerted C–C or C–X reductive elimination reactions.[53,54] However, all such models had calculated activation energies that were too high to be consistent with the experimental data. Finally, it was found that addition of an external nucleophile to form a hydrogen bond with the PdOH group of **3′** led to the prediction of a lower activation energy, perhaps by introducing oxopalladium(IV) character to the PdOH group (compare Scheme 2 [15]). Evidently, since complex **1** and **2** exhibit the same reactivity, the pendent OH of ligand **L1** cannot serve this role *via* a more facile intramolecular pathway. The $(CH_2)_3OH$ substituent is likely positioned too far away to be of assistance, since the tertiary amine donor is *trans* to the PdOH group in the calculated structure **3′·OH**. Fig. 8 illustrates the reductive elimination mechanism with hydroxide as the external nucleophile, but it could also be solvent dmso or water. Typical of overall reductive elimination from octahedral palladium(IV) or platinum(IV) complexes,[53,54] several steps are involved in the conversion of Pd(IV)–OH (**3′**) to Pd(II)–OH (**5′**) and organic product (**BP**). The reaction is predicted to lead initially to the product of oxygen atom insertion, with a hydrogen bonded water molecule, ***R***. In the transition state both the Pd–N(amine) and Pd–N(py *trans* to aryl) bond distances lengthened, corresponding to partial dissociation, while the O–C(aryl) bond was formed, and the Pd–C(aryl) bond was cleaved. Thus, from **3′·OH** to the transition state the Pd–C(Ar) bond distance increased from 2.05 Å to 2.14 Å, the O···C(Ar) distance decreased from 3.00 Å to 2.36 Å, and the O–Pd–C(Ar) angle decreased from 95.0° to 69.2° (Fig. 8). The reductive elimination from **3′·OH** is therefore concerted, and this was also the optimal calculated mechanistic pathway for related palladium neophyl complexes supported by exclusively bidentate diimine ligands.[16] The further hydrolysis of ***R*** then leads to the hydroxopalladium(II) product **5′** and *t*-butylphenol, **BP**. High selectivity for **BP** generated by O–C_{Ar} bond formation is favoured for an innersphere concerted reductive elimination mechanism of the present and prior[16] studies. In contrast,

Published on 13 Haziran 2024. Downloaded on 8.08.2024 12:38:59.

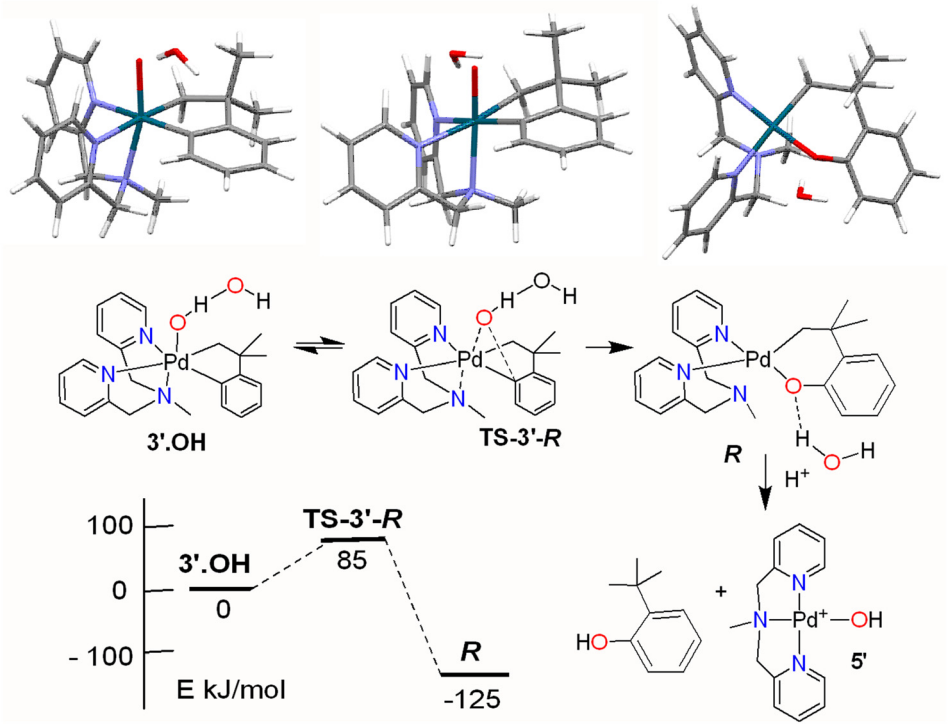

Fig. 8 The calculated structures and relative energies (*E*, kJ mol^{-1}) for reductive elimination from model complex **3′·OH** to give intermediate ***R***. Calculated bond parameters: **3′·OH**, Pd–C(Ar) 2.05, Pd–O 2.01, O···C(Ar) 3.00, Pd–N 2.31, Pd-py(t-Ar) 2.20, PdO–H 1.37, PdOH–O 1.15 Å, O–Pd–C (Ar) 95.0°; **TS-3′-*R***, Pd–C(Ar) 2.14, Pd–O 2.01, O···C(Ar) 2.36, Pd–N 2.36, Pd-py(t-Ar) 2.36, PdO–H 1.40, PdOH–O 1.11 Å, O–Pd–C (Ar) 69.2°; ***R***, Pd···C(Ar) 2.94, Pd–O 2.07, O–C(Ar) 1.38, Pd–N 2.74, Pd-py(t-O) 2.09, PdO–H 1.69, PdOH–O 1.02 Å, O–Pd–C(Ar) 25.3°.

external attack by $^{-}$OR nucleophiles has previously been shown to give selective alkyl–oxygen bond formation.[19]

3. Conclusions

Rare examples of hydroxopalladium(IV) complexes, **3** and **4**, formed by oxidative addition using hydrogen peroxide or oxygen as oxidants, are reported. The ligands **L1** and **L2** each contain three nitrogen-donor groups while **L1** also contains a pendent hydroxyl group. In both the oxidation reactions (Scheme 5) and the reduction reactions (Scheme 6), the palladium complexes containing **L1** and **L2** show similar reactivity, and so it seems that the presence of the third nitrogen donor is more important than the potential hydrogen bonding hydroxyl substituent in the ligands. The reductive elimination from the new palladium(IV) complexes is selective for aryl–oxygen bond formation, and a concerted mechanism is proposed. Similar reactivity is observed through the sequential oxidative addition and reductive elimination with palladium complexes supported by rigorously bidentate ligands. Thus, **3** and **4** are good models for the high valent intermediates due to the hemilability of **L1**/**L2**.

DFT calculations indicate that the oxidation reactions have a low energy barrier, mostly associated with the rearrangement of the precursor reagent **1** or **2** to the less stable isomer **1c** or **2c** (Fig. 5) prior to reaction with H_2O_2 or O_2/H_2O (Scheme 5 and Fig. 6 and 7). Oxidation *via* this isomer means that the pendent hydroxyl group in **L1** is positioned too far away from the Pd–oxygen moieties to assist in any oxidation steps *via* hydrogen bonding. This explains why complex **1** supported by **L1** has indistinguishable reactivity to complex **2**, bearing a pendent methoxy group, which should not engage in second coordination sphere assistance. The calculations predict that the reductive elimination from **3** or **4** involves several steps. As the C–O bond forms, the proton of the original PdOH group becomes more acidic, as it takes on the character of a coordinated phenol, and it is transferred to an adjacent basic site. Ultimately, it protonates the Pd–CH_2 bond leading to Pd–CH_2 protolysis. Together, these results add significantly to the understanding of the factors that promote oxidation of organopalladium(II) complexes by dioxygen, and the factors that allow organopalladium(IV) complexes, often invoked as short-lived reaction intermediates in stoichiometric or catalytic reactions, to be studied directly.

4. Experimental

NMR spectra were recorded using a Varian INOVA 600 MHz spectrometer. ^{1}H and ^{13}C chemical shifts were referenced internally to solvent (residual signal for ^{1}H) where the chemical shift was set to appropriate values relative to TMS at 0.00 ppm. Complete assignment of each compound was aided

 This journal is © The Royal Society of Chemistry 2024

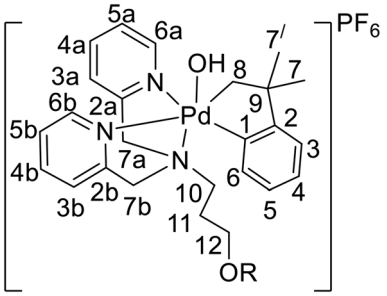

3, R = H
4, R = Me

Scheme 7 NMR labels for Pd(IV) complexes **3** and **4**.

Published on 13 Haziran 2024. Downloaded on 8.08.2024 12:38:59.

by the use of ^{1}H–^{1}H gCOSY, ^{1}H–^{13}C{^{1}H} HSQC and ^{1}H–^{13}C{^{1}H} HMBC experiments and are reported using the labeling shown in Scheme 7. Commercial reagents and aqueous 30% H_2O_2 were used without further purification. The palladium(II) precursor complexes **1** and **2**[16] and the ligands **L1** and **L2**[30,31] were synthesized according to the literature procedures. Dioxygen (99%) was purchased from Praxair and passed through a drying tube containing calcium sulphate and a cold ice trap to remove water prior to use.

The DFT calculations were carried out using the programs implemented in AMS2023.[50] The BLYP functional was used, with double-zeta basis set and first-order scalar relativistic corrections.[55] The solvent effects were modeled by using COSMO.[56] The NEB (nudged elastic band) method was used for finding the minimum energy reaction paths, because this method can roughly track the reaction coordinate and gives good insight into reaction mechanism.[57–59] Details of the calculated ground state and transition state structures are given in the ESI.†

The single crystals for structure determination were mounted on a Mitegen polyimide micromount with a small amount of Paratone N oil. All X-ray measurements were made by using a Bruker Kappa Axis Apex2 diffractometer at a temperature of 110 K (ref. 60 and 61) and structures were determined and refined by using the SHELX programs.[62,63] Details are given in the cif files (CCDC 2091353, 2091354, 2334979†).

4.1. [Pd(OH)($CH_2CMe_2C_6H_4$)(κ^3-*N,N′,N″*-L1)][PF_6], 3

Method A. Dioxygen was bubbled through a stirred solution of complex **1** ((0.300 g, 0.631 mmol) in MeOH (10 mL) at 0 °C) for 5 min, followed by addition of NH_4PF_6 (0.308 g, 1.89 mmol) and further stirring under O_2 for 10 min. The yellow precipitate of the product which formed was separated by filtration, washed with cold MeOH (10 mL) and diethyl ether (20 mL) and dried under vacuum. Yield: 0.282 g, 0.428 mmol, 71%.

Method B. To a stirred solution of complex **1** (0.060 g, 0.126 mmol) in $CDCl_3$ (3 mL) cooled to 8 °C was added excess NH_4PF_6 (0.061 g, 0.378 mmol) and then H_2O_2 (11.6 μL, 0.7 mmol) and the mixture was stirred for 15 min. The yellow precipitate of the product **3** was isolated as above. Yield: 0.033 g, 0.050 mmol, 40%. ^{1}H NMR (600 MHz, dmso-d_6): δ = 8.72 (d, 1H, J = 5 Hz, *H6b*), 8.57 (d, 1H, J = 5 Hz, *H6a*), 7.98 (t, 1H, J = 8 Hz, *H4b*), 7.94 (t, 1H, J = 8 Hz, *H4a*), 7.56–7.52 (m, 2H, *H3b* and *H5b*), 7.50 (dd, 1H, J = 5 Hz, 8 Hz, *H5a*), 7.46 (d, 1H, J = 8 Hz, *H3a*), 7.11 (t, 1H, J = 7 Hz, *H5*), 7.05 (d, 1H, J = 7 Hz, *H6*), 6.90 (t, J = 7 Hz, 1H, *H4*), 6.63 (d, 1H, J = 7 Hz, *H3*), 4.92 (d, 1H, J = 17 Hz, *H7a*), 4.58–4.62 (m, 2H, H7a′, H7b′), 4.52 (d, 1H, J = 16 Hz, *H7b*), 4.04 (d, 1H J = 7 Hz, *H8′*), 4.01 (d, 1H, J = 7 Hz, *H8*), 3.35 (m, 1H, *H12*), 3.33 (m, 1H, *H10*), 3.29 (m, 1H, *H10′*), 2.45 (m, 1H, *H12′*), 1.86 (m, 1H, *H11*), 1.78 (m, 1H, *H11′*), 1.43 (s, 6H, *H7*, *H7′*); ^{13}C{^{1}H} NMR (151 MHz, dmso-d_6): δ = 160.56 (*C*2), 156.99 (*C*2a), 155.66 (*C*2b), 153.46 (*C*1), 145.45 (*C*6b), 145.10 (*C*6a), 140.04 (*C*4b), 139.93 (*C*4a), 129.95 (*C*3), 126.96 (*C*4), 126.02 (*C*5), 125.58 (*C*6), 124.67 (*C*3b and *C*5b), 124.32 (*C*5a), 123.03 (*C*3b and *C*5b), 122.24 (*C*3a), 66.13 (*C*7b), 65.77 (*C*7a), 65.37 (*C*8), 61.68 (*C*12), 58.16 (*C*10), 47.11 (*C*9), 34.67 (*C*7′), 31.13 (*C*7), 23.50 (*C*11).

4.2. [Pd(OH)($CH_2CMe_2C_6H_4$)(κ^3-*N,N′,N″*-L2)][PF_6], 4

This was prepared in a similar way as for complex **3**, but by using complex **2** as reagent. Yield by Method A: 62%; yield by Method B: 30%. ^{1}H NMR (600 MHz, CD_2Cl_2): δ = 8.75 (d, 1H, J = 5 Hz, *H6b*), 8.58 (d, 1H, J = 5 Hz, *H6a*), 7.79 (t, 1H, J = 8 Hz, *H4a*), 7.58 (t, 1H, J = 8 Hz, *H4b*), 7.54 (d, 1H, J = 8 Hz, *H*3b), 7.43–7.40 (m, 2H, *H5b*, *H3a*), 7.39 (dd, 1H, J = 5 Hz, 8 Hz, *H5a*), 7.17 (t, 1H, J = 7 Hz, *H4*), 7.04 (t, 1H, J = 7 Hz, *H6*), 6.92 (t, 1H, J = 7 Hz, *H5*), 6.67 (d, J = 7 Hz, 1H, *H3*), 4.62–4.42 (m, 4H, *H7a*, *H7a′*, *H7b*, *H7b′*), 4.24 (d, 1H J = 7 Hz, *H8′*), 3.90 (d, 1H, J = 7 Hz, *H8*), 3.38 (m, 1H, *H12*), 3.33 (m, 1H, *H10*), 3.17 (s, 3H, OCH_3), 3.14 (m, 1H, *H10′*), 2.57 (m, 1H, *H12′*), 2.05 (m, 1H, *H11*), 1.88 (m, 1H, *H11′*), 1.48 (s, 3H, *H7*), 1.46 (s, 3H, *H7′*); ^{13}C{^{1}H} NMR (151 MHz, CD_2Cl_2): δ = 160.73 (*C*2), 156.08 (*C*2a) 154.78 (*C*2b), 152.93 (*C*1), 145.91 (*C*6b), 145.67 (*C*6a), 140.24 (*C*4a), 140.21 (*C*4b), 130.04 (*C*3), 127.81 (*C*5), 127.06 (*C*4), 126.48 (*C*6), 125.16 (*C*5b), 124.84 (*C*5a), 123.57 (*C*3b), 122.81 (*C*3a), 69.29 (*C*10), 67.34 (*C*8), 66.63 (*C*7a), 66.50 (*C*7b), 63.15 (*C*12), 58.51 (OCH_3), 46.98 (*C*9), 31.16 (*C*7′), 31.10 (*C*7), 22.90 (*C*11). HR ESI-TOF MS: Calcd for [$C_{26}H_{34}N_3O_2Pd$]$^+$: m/z = 526.1685 Obsd m/z = 526.1690. Single crystals suitable for single-crystal X-ray crystallographic analysis were grown from acetone/ether at −15 °C.

4.3. [Pd(OH)(κ^3-*N,N′,N″*-L2)][PF_6], 5

A solution of complex **4** (0.060 g 0.089 mmol) in dmso-d_6 (0.5 mL), with 1,3,5-trimethoxybenzene as internal standard, in an NMR tube was heated at 110 °C for 1.5 h. ^{1}H NMR (600 MHz, dmso-d_6): δ = 9.28 (br s, 1H, O*H*), 8.62 (d, 2H, J = 5 Hz, *H6a*), 8.02 (t, 2H, J = 7 Hz, *H4a*), 7.57 (d, 2H, J = 7 Hz, *H3a*), 7.45 (dd, 2H, J = 7 Hz, 5 Hz, *H5a*), 4.89 (d, 2H, J = 15 Hz, *H7a*), 4.22 (d, 2H, J = 15 Hz, *H7a′*), 2.98 (s, 3H, O*Me*), 3.10 (m, 2H, *H10*), 3.07 (m, 2H, *H12*), 1.51 (m, 2H, *H11*); 2-*t*-butylphenol, **BP**, δ(^{1}H) = 7.21 (d, 1H, J = 7 Hz, *H3*), 6.71 (t, 1H, J = 7 Hz, *H5*), 6.55 (t, 1H, J = 7 Hz, *H4*), 6.49 (d, 1H, J = 7 Hz, *H6*), 1.37 (s, 9H, *t*-Bu). Yields by NMR integration against internal standard: **5**, 94%; **BP**, 86%; **BPC**, 9%. The identity of **BP** and **BPC** were confirmed by GC-MS analysis.

Published on 13 Haziran 2024. Downloaded on 8.08.2024 12:38:59.

4.4. [PdCl(κ³-*N,N′,N″*-L2)][PF_6], 6

A solution of complex **4** (0.060 g 0.089 mmol) in $CHCl_3$ (5 mL) was heated at 55 °C for 8 h. On cooling, a yellow precipitate was formed. The precipitate was collected by filtration and washed with ether (3 × 5 mL) and hexane (3 × 5 mL) to give complex **6**. Yield: 0.026 g, 0.048 mmol, 54%. ^{1}H NMR (600 MHz, dmso-d_6): δ = 8.59 (d, 2H, J = 5 Hz, *H6a*), 8.22 (t, 2H, J = 7 Hz, *H4a*), 7.75 (d, 2H, J = 7 Hz, *H3a*), 7.65 (dd, 2H, J = 7 Hz, 5 Hz, *H5a*), 5.50 (d, 2H, J = 15 Hz, *H7a*), 4.50 (d, 2H, J = 15 Hz, *H7a′*), 3.29 (m, 2H, *H*10), 3.12 (s, 3H, O*Me*), 3.07 (m, 2H, *H*12), 1.83 (m, 2H, *H*11); ^{13}C{^{1}H} NMR (151 MHz, dmso-d_6): δ = 165.41 (*C*2a), 150.71 (*C*6a), 124.09 (*C*4a), 125.58 (*C*3a), 123.84 (*C*5a), 69.18 (*C*10), 67.29 (*C*7a), 60.86 (*C*12), 58.33 (OCH_3), 28.14 (*C*11). To characterize the organic products, an analogous reaction mixture was filtered through a plug of silica to remove the palladium complexes, then the solvent was evaporated from the filtrate and the product mixture was used for GC-MS analysis.

4.5. [PdCl($CH_2CMe_2C_6H_4$)(κ³-*N,N′,N″*-L2)][PF_6], 7

A sample of complex **4** (0.04 g), prepared from **2** and H_2O_2 as above, was dissolved in $CHCl_3$ (10 mL) and the solution was layered with ether (15 mL). Slow diffusion over 1 week at room temperature led to formation of yellow crystals of complex **7**. Yield 0.016 g, 39%. ^{1}H NMR (600 MHz, CD_2Cl_2): δ = 8.87 (d, 1H, J = 5 Hz, *H6b*), 8.76 (d, 1H, J = 5 Hz, *H6a*), 7.83 (d, 1H, J = 8 Hz, *H3b*), 7.63 (t, 1H, J = 8 Hz, *H4a*), 7.40 (dd, 1H, J = 8 Hz, 5 Hz, *H5b*), 7.31 (dd, 1H, J = 8 Hz, 5 Hz, *H5a*), 7.10 (t, 1H, J = 7 Hz, *H*5), 7.02 (t, 1H, J = 7 Hz, *H*6), 6.95 (t, 1H, J = 7 Hz, *H*4), 6.65 (d, 1H, J = 7 Hz, *H*3), 5.98, 4.70 (each 1H, d, J = 17 Hz, *H7a*, *H7a′*), 5.79, 4.31 (each 1H, d, J = 15 Hz, *H7b*, *H7b′*), 4.42, 3.90 (each 1H, d, J = 8 Hz, *H*8, *H*8′), 3.3 (m, 2H, *H*12, *H*12′), 3.25, 3.12 (each m, 1H, *H*10, *H*10′), 3.17 (s, 3H, *OMe*), 2.30, 2.01 (each m, 1H, *H*11, *H*11′), 1.48, 1.46 (each s, 3H, *H*7, *H*7′). HR ESI-TOF MS: Calcd for $[C_{26}H_{33}ClN_3O_2Pd]^+$: m/z = 544.1347 Obsd. m/z = 544.1328.

Data availability

All data may be obtained on request to the corresponding author (JMB or RJP).

Conflicts of interest

There are no conflicts to declare.

Acknowledgements

We thank the NSERC (Canada) for financial support.

References

1 S. Moghimi, M. Mahdavi, A. Shafiee and A. Foroumadi, *Eur. J. Org. Chem.*, 2016, 3282–3299.
2 J. Le Bras and J. Muzart, *Eur. J. Org. Chem.*, 2018, 1176–1203.
3 H. Sterckx, B. Morel and B. U. W. Maes, *Angew. Chem., Int. Ed.*, 2019, **58**, 7946–7970.
4 A. N. Campbell and S. S. Stahl, *Acc. Chem. Res.*, 2012, **45**, 851–863.
5 Z. Zhuang, A. N. Herron, Z. Fan and J.-Q. Yu, *J. Am. Chem. Soc.*, 2020, **142**, 6769–6776.
6 J. M. Racowski, N. D. Ball and M. S. Sanford, *J. Am. Chem. Soc.*, 2011, **133**, 18022–18025.
7 M. C. Denney, N. A. Smythe, K. L. Cetto, R. A. Kemp and K. I. Goldberg, *J. Am. Chem. Soc.*, 2006, **128**, 2508–2509.
8 B. V. Popp and S. S. Stahl, *J. Am. Chem. Soc.*, 2007, **129**, 4410–4422.
9 N. R. Deprez and M. S. Sanford, *Inorg. Chem.*, 2007, **46**, 1924–1935.
10 J. Zhang, E. Khaskin, N. P. Anderson, P. Y. Zavalij and A. N. Vedernikov, *Chem. Commun.*, 2008, 3625–3627, DOI: **10.1039/B803156H**.
11 Y.-H. Zhang and J.-Q. Yu, *J. Am. Chem. Soc.*, 2009, **131**, 14654–14655.
12 H. Zhu, P. Chen and G. Liu, *J. Am. Chem. Soc.*, 2014, **136**, 1766–1769.
13 K. J. Stowers, A. Kubota and M. S. Sanford, *Chem. Sci.*, 2012, **3**, 3192–3195.
14 K. J. Stowers, K. C. Fortner and M. S. Sanford, *J. Am. Chem. Soc.*, 2011, **133**, 6541–6544.
15 P. L. Alsters, H. T. Teunissen, J. Boersma, A. L. Spek and G. van Koten, *Organometallics*, 1993, **12**, 4691–4696.
16 A. Behnia, P. D. Boyle, J. M. Blacquiere and R. J. Puddephatt, *Organometallics*, 2016, **35**, 2645–2654.
17 A. J. Canty, H. Jin, B. W. Skelton and A. H. White, *Inorg. Chem.*, 1998, **37**, 3975–3981.
18 W. Oloo, P. Y. Zavalij, J. Zhang, E. Khaskin and A. N. Vedernikov, *J. Am. Chem. Soc.*, 2010, **132**, 14400–14402.
19 A. J. Canty, A. Ariafard, N. M. Camasso, A. T. Higgs, B. F. Yates and M. S. Sanford, *Dalton Trans.*, 2017, **46**, 3742–3748.
20 J. T. Groves and G. A. McClusky, *J. Am. Chem. Soc.*, 1976, **98**, 859–861.
21 X. Huang and J. T. Groves, *JBIC, J. Biol. Inorg. Chem.*, 2017, **22**, 185–207.
22 A. J. Canty, H. Jin, A. S. Roberts, B. W. Skelton and A. H. White, *Organometallics*, 1996, **15**, 5713–5722.
23 F. Qu, J. R. Khusnutdinova, N. P. Rath and L. M. Mirica, *Chem. Commun.*, 2014, **50**, 3036–3039.
24 A. V. Sberegaeva, P. Y. Zavalij and A. N. Vedernikov, *J. Am. Chem. Soc.*, 2016, **138**, 1446–1455.
25 A. J. Canty, *Dalton Trans.*, 2009, 10409–10417, DOI: **10.1039/B914080H**.

This journal is © The Royal Society of Chemistry 2024

Published on 13 Haziran 2024. Downloaded on 8.08.2024 12:38:59.

26 P. Sehnal, R. J. K. Taylor and I. J. S. Fairlamb, *Chem. Rev.*, 2010, **110**, 824–889.
27 J. W. Schultz, N. P. Rath and L. M. Mirica, *Inorg. Chem.*, 2020, **59**, 11782–11792.
28 D. J. Nelson and S. P. Nolan, *Coord. Chem. Rev.*, 2017, **353**, 278–294.
29 L. M. Martínez-Prieto and J. Cámpora, *Isr. J. Chem.*, 2020, **60**, 373–393.
30 K. Sundaravel, M. Sankaralingam, E. Suresh and M. Palaniandavar, *Dalton Trans.*, 2011, **40**, 8444–8458.
31 J.-Z. Wu, E. Bouwman, A. M. Mills, A. L. Spek and J. Reedijk, *Inorg. Chim. Acta*, 2004, **357**, 2694–2702.
32 J. Cámpora, J. A. López, P. Palma, P. Valerga, E. Spillner and E. Carmona, *Angew. Chem., Int. Ed.*, 1999, **38**, 147–151.
33 J. Cámpora, P. Palma and E. Carmona, *Coord. Chem. Rev.*, 1999, **193**, 207–281.
34 A. Behnia, M. A. Fard, J. M. Blacquiere and R. J. Puddephatt, *Organometallics*, 2017, **36**, 4759–4769.
35 A. Behnia, P. D. Boyle, M. A. Fard, J. M. Blacquiere and R. J. Puddephatt, *Dalton Trans.*, 2016, **45**, 19485–19490.
36 A. Behnia, M. A. Fard, J. M. Blacquiere and R. J. Puddephatt, *Organometallics*, 2020, **39**, 4037–4050.
37 M. A. Fard, A. Behnia and R. J. Puddephatt, *Organometallics*, 2017, **36**, 4169–4178.
38 A. Abo-Amer, P. D. Boyle and R. J. Puddephatt, *Inorg. Chim. Acta*, 2020, **507**, 119580.
39 H. W. Roesky, S. Singh, K. K. M. Yusuff, J. A. Maguire and N. S. Hosmane, *Chem. Rev.*, 2006, **106**, 3813–3843.
40 T. Steiner, *Angew. Chem., Int. Ed.*, 2002, **41**, 48–76.
41 J. Hine, *J. Am. Chem. Soc.*, 1950, **72**, 2438–2445.
42 H. C. Brown and M. D. Taylor, *J. Am. Chem. Soc.*, 1947, **69**, 1332–1336.
43 R. Spitzer and K. S. Pitzer, *J. Am. Chem. Soc.*, 1948, **70**, 1261–1264.
44 L. Sacconi and G. Lombardo, *J. Am. Chem. Soc.*, 1960, **82**, 6266–6269.
45 A. Behnia, M. A. Fard and R. J. Puddephatt, *J. Organomet. Chem.*, 2019, **902**, 120962.
46 K. A. Thompson, C. Kadwell, P. D. Boyle and R. J. Puddephatt, *J. Organomet. Chem.*, 2017, **829**, 22–30.
47 M. E. Moustafa, P. D. Boyle and R. J. Puddephatt, *Chem. Commun.*, 2015, **51**, 10334–10336.
48 E. M. Prokopchuk, H. A. Jenkins and R. J. Puddephatt, *Organometallics*, 1999, **18**, 2861–2866.
49 V. V. Rostovtsev, L. M. Henling, J. A. Labinger and J. E. Bercaw, *Inorg. Chem.*, 2002, **41**, 3608–3619.
50 B. V. Popp, J. E. Wendlandt, C. R. Landis and S. S. Stahl, *Angew. Chem., Int. Ed.*, 2007, **46**, 601–604.
51 C. R. Landis, C. M. Morales and S. S. Stahl, *J. Am. Chem. Soc.*, 2004, **126**, 16302–16303.
52 K. M. Gligorich and M. S. Sigman, *Angew. Chem., Int. Ed.*, 2006, **45**, 6612–6615.
53 A. J. Canty, *Acc. Chem. Res.*, 1992, **25**, 83–90.
54 R. J. Puddephatt, *Angew. Chem., Int. Ed.*, 2002, **41**, 261–263.
55 A. D. Becke, *Phys. Rev. A*, 1988, **38**, 3098–3100.
56 J. Andzelm, C. Kölmel and A. Klamt, *J. Chem. Phys.*, 1995, **103**, 9312–9320.
57 G. Henkelman, B. P. Uberuaga and H. Jónsson, *J. Chem. Phys.*, 2000, **113**, 9901–9904.
58 G. Henkelman and H. Jónsson, *J. Chem. Phys.*, 2000, **113**, 9978–9985.
59 E. Bitzek, P. Koskinen, F. Gähler, M. Moseler and P. Gumbsch, *Phys. Rev. Lett.*, 2006, **97**, 170201.
60 Bruker-Nonius, *SAINT, version and 2013.8*, Bruker-Nonius, Madison, WI 53711, USA, 2013.
61 Bruker-Nonius, *SADABS, version and 2012.1*, Bruker-Nonius, Madison, WI 53711, USA, 2012.
62 G. M. Sheldrick, *Acta Crystallogr., Sect. A: Found. Adv.*, 2015, **71**, 3–8.
63 G. M. Sheldrick, *Acta Crystallogr., Sect. C: Struct. Chem.*, 2015, **71**, 3–8.